Molecular Modification of Transient Receptor Potential Canonical 6 Channels Modulates Calcium Dyshomeostasis in a Mouse Model Relevant to Malignant Hyperthermia

Jose R Lopez MD, PhD[1,2], Arcady Uryash MD, PhD[3], Jose Adams, MD[3], Philip M Hopkins MD FRCA[4], Paul D Allen MD, PhD[1,4&]

[1]Department of Molecular Biosciences, University of California Davis,
Davis, CA 95616, USA.
[2]Department of Research, Mount Sinai Medical Center,
Miami Beach, FL 33140, USA.
[3]Department of Neonatology, Mount Sinai Medical Center,
Miami Beach, FL 33140, USA.
[4]Institute of Medical Research at St James's, University of Leeds,
Leeds, LS9 7TF United Kingdom.

[&]Corresponding Author: Paul D Allen, Malignant Hyperthermia Investigation Unit, St James' University Hospital, Leeds, LS9 7TF United Kingdom, Email: p.d.allen@leeds.ac.uk

Clinial Trial Number (not applicable)

Word and Element Counts: Number of words in Abstract **299**, in Introduction **336** and in Discussion **1144**; number of figures **9**; number of tables None; number of appendices **2**; and number of supplementary files 2

Running Title: **TRPC6 modulation in Malignant Hyperthermia**

Summary Statement: (not applicable)

Funding Statement: National Institute of Arthritis, Musculoskeletal and Skin Diseases (1R01AR068897; P.D.A., P.M.H., J.R.L.); National Institute of Arthritis, Musculoskeletal and Skin Diseases (P01AR-05235; P.D.A., J.R.L., P.M.H.); AFM-Téléthon-France (21543; J.R.L.), Florida Heart Foundation (J.R.L., A.U. J.A)

Conflicts of Interest The authors declare that they have no conflicts of interest with the contents of this article[1]

Abstract.

[1] The content is solely the responsibility of the authors and does not necessarily represent the official views of the National Institutes of Health or the Medical Research Council

Background: We have previously shown using pharmacologic modulation that Transient Receptor Potential Cannonical (TRPCs) channels play an important role in the pathogenesis of malignant hyperthermia. Here we tested the hypothesis that genetically supressing the function of TRPC6 can partially ameliorate muscle cation dyshomeostasis and the response to halothane in a mouse model relevant to malignant hyperthermia.

Methods: We studied the effect of overexpressing a muscle specific non-conducting dominant negative TRPC6 channel in 20 *RYR1*-p.R163C and 20 wild-type mice and an equal number of non-expressing controls, using calcium and sodium selective microelectrodes and Western blots.

Results: *RYR1*-p.R163C mouse muscles have chronically elevated intracellular calcium and sodium levels compared to wild type muscles. Transgenic expression of the non-conducting TRPC6 channel reduced intracellular calcium from 331±34 nM (mean±SD) to 190±27 nM, $p<0.0001$ and sodium from 15±1mM to 11±1mM ($p<0.0001$). Its expression lowered the increase in intracellular Ca^{2+} of the TRPC6 specific activator hyperforin in *RYR1*-p.R163C muscle fibers from 52% (348±37nM to 537±70nM) to 14% (185±11nM, to 210±44nM). Western blot analysis of TRPC3 and TRPC6 expression showed the expected increase in TRPC6 due to overexpression of its dominant negative transgene and a compensatory increase in expression of TRPC3. Although expression of the muscle-specific dominant negative TRPC6 was able to modulate the increase in intracellular calcium during halothane exposure and prolonged life (35±5 min *vs* 15±3 min, $p<0.0001$), a slow steady increase in calcium began after 20 min of halothane exposure which eventually led to death.

Conclusions: These data support our previous findings that TRPC channels play an important role in causing the intracellular calcium and sodium dyshomeostasis associated with *RYR1* variants that are pathogenic for malignant hyperthermia. However they also show that modulating TRPC channels alone is not sufficient to prevent the lethal effect of exposure to volatile anesthetic malignant hyperthermia triggering agents.

Introduction.

Malignant hyperthermia (MH) is an autosomal dominant hypermetabolic condition triggered by volatile anesthetics, such as isoflurane, and succinylcholine[1-4]. Molecular genetic studies have established the type 1 ryanodine receptor gene (*RYR1*) encoding the skeletal muscle sarcoplasmic reticulum Ca^{2+} release channel as the primary locus for both MH susceptibility and central core disease[2-6]. A common characteristic of muscle expressing MH-*RYR1* variants, both in patients[7] and in experimental models[8-12], is an increased intracellular Ca^{2+} concentration compared to muscle from non-susceptible subjects. In three experimental murine models of MH with variants in *RYR1* that are known to be pathogenic in humans, we have shown that exposure to halothane or isoflurane at clinically relevant concentrations causes intracellular Ca^{2+} concentration to rise several fold in their muscles, whereas exposure to the same concentrations of halothane or isoflurane has no effect in muscles from mice without *RYR1* variants[10-12]. Previously, we introduced a new paradigm that implicates nonspecific sarcolemmal cation entry via transient receptor potential canonical (TRPC) channels both as the predominant source of acutely elevated intracellular Ca^{2+} and Na^{+} concentration during fulminant MH and as important contributors to chronically elevated intracellular Ca^{2+} and Na^{+} concentrations in quiescent MH-susceptible muscles[13,14].

Our aim in this study was to use molecular methods in combination with pharmacologic agents to further test the primary hypothesis that TRPC3 and TRPC6 channels are directly responsible for both the high intracellular Ca^{2+} concentration seen in resting MH susceptible muscles, with a secondary hypothesis that blocking TRPC6 could prevent the massively elevated intracellular Ca^{2+} concentration observed during the

MH crisis following exposure to triggering agents and subsequent death. We have done this using our *RYR1*-p.R163C knock-in murine model of MH[10] crossed with a transgenic animal overexpressing a dominant negative non-conducting TRPC6 channel in their skeletal muscles[15,16]. This transgene exerts its effect by blocking the activity of TRPC6 and perhaps also by modulating TRPC3 because these two closely related TRPC channel isoforms are known to form hetero-tetramers at the plasma membrane[17]. A previous study in two murine models of muscular dystrophy, expressing this non-conducting channel relieved their muscle pathology, and restored muscle function to near normal levels[15].

Material and Methods.-

Animals

The animals used in this study were: i) Wild type C57BL/6J mice; ii) C57BL/6J knock-in mice heterozygous for the *RYR1* variant resulting in the amino acid change p.R163C in the RyR1 protein (R163C); iii) Transgenic mice with skeletal muscle-specific overexpression of a non-conducting TRPC6 channel[15]; or iv) Mice heterozygous for *RYR1*-p.R163C with skeletal muscle-specific expression of a non-conducting TRPC6 channel (the result of crossing *RYR1*-p.R163C with mice with skeletal muscle-specific expression of a non-conducting TRPC6 channel). Mice were used as close to the time they achieved 3 months of age. In all, 91 mice (39 females and 52 males) were used as experimental animals. Animals for any phase of the study were chosen by their date of birth (oldest first) and their availability in the animal colony. All experimental procedures on animals were in accordance with the Care and Use Handbook of Laboratory Animals published by the US National Institute of Health (NIH publication No. 85-23, revised 1996) and approved by the Institutional Animal Care and Use Committees at the University of California at Davis, Davis CA, the Mount Sinai Hospital, Miami Beach FL and the Home Office in the United Kingdom.

Experimental Preparations.-

Experiments were conducted either: *(i) in vitro* using single muscle fibers obtained by enzymatic digestion of *flexor digitorum brevis* muscles dissected from 3-5-month-old anesthetized mice killed by cervical dislocation[18]. *Flexor digitorum brevis* fibers were used for measurements of intracellular ion concentrations 4-6 h after isolation; or *(ii) In vivo*, by measurement of intracellular ion concentrations in surgically exposed *vastus lateralis*

fibers of mice anesthetized using a mixture of intraperitoneal ketamine (100 mg/kg) and xylazine (5 mg/kg)[13].

$Ca^{2+}$and Na^{+}-selective microelectrodes.-

Double-barreled Ca^{2+} and Na^{+} selective microelectrodes were prepared and individually calibrated before and after the determination of intracellular calcium concentration or intracellular sodium concentration as described previously[13,19]. Only those Ca^{2+} selective microelectrodes with a linear relationship between pCa 3 and 7 (Nernstian response 30.5 mV/pCa unit at 37°C) or those Na^{+} microelectrode with Nernstian responses between 100 and 10 mM, and a sub-Nernstian response (40–45 mV) between 1 and 10 mM were used experimentally. The sensitivity of neither the Ca^{2+} nor Na^{+} selective microelectrodes were affected by any of the drugs used in the present study. After making measurements of $[Ca^{2+}]_r$ and $[Na^{+}]_r$ all microelectrodes were recalibrated, and if the two calibration curves did not agree within 5 mV, data from that microelectrode were discarded. This resulted in the removal of the data of 11 animals from the final analysis.

Recording of intracellular Ca^{2+} and Na^{+} in muscle fibers in vitro and in vivo.-

Intracellular Ca^{2+} and Na^{+} determinations were performed *in vitro,* on single *flexor digitorum brevis* muscle fibers as described previously[18], and *in vivo*, on *vastus lateralis* fibers in anesthetized MHN and MHS mice[10]. Muscle fibers were impaled with double-barreled Ca^{2+}-selective or Na^{+}-selective microelectrodes, and their potentials were recorded via a high-impedance amplifier (WPI Duo 773 electrometer; WPI, Sarasota, FL, USA)[10]. Data was not collected in any muscle cell whose membrane potential was more positive than -80mV and if that occurred at any time during the experiment the data for

that cell was not used for analysis.

The resting membrane potential from the 3 M KCl microelectrode was subtracted electronically from either the potential of the Ca^{2+} microelectrode, or the Na^{+} microelectrode to produce a differential Ca^{2+}- specific potential or Na^{+}-specific potential that represents the intracellular Ca^{2+}or intracellular Na^{+} concentrations, respectively. All voltage signals were stored in a computer for further analysis.

Solutions. -

Normal Ringer solution contained (in mM): 135 NaCl, 5 KCl, 1.8 $CaCl_2$, 1 $MgCl_2$, 18 $NaHCO_3$, 1.5 NaH_2PO, and 5 glucose, pH 7.2–7.3. 1-oleoyl-2-acetyl-*sn*-glycerol (OAG), ethyl-1-(4-(2,3,3-trichloroacrylamide)phenyl)-5-(trifluoromethyl)-1H-pyrazole-4-carboxylate and hyperforin solutions were made by adding the desired concentration of the reagent to normal Ringer solution. All in vitro experiments were performed at 37°C.

Halothane Survival Curve.-

To investigate the effects of overexpressing a dominant-negative non-conducting TRPC6 in *RYR1*-p.R163C mice on the response to exposure to 2% halothane, we conducted a survival study on cohorts (N_{mice}= 7/group) of 8-12-week-old wild type, wild type/dominant negative TRPC6, *RYR1*-p.R163C, and *RYR1*-p.R163C/dominant negative TRPC6 mice. Survival time was measured during an up to 60 min exposure to 2% halothane.

Western blot analysis of protein expression.-

Gastrocnemius muscles from all genotypes were dissected, minced and homogenized in modified radioimmunoassay precipitation assay (RIPA) buffer as described before[20]. Total protein concentration was determined using the Pierce BCA

Protein Assay Kit (Thermo-Scientific, MA, USA). Proteins were separated on SDS gel, transferred to nitrocellulose membrane. To avoid having the errors added by attempting to measure all of the proteins on a single gel, by stripping the antibodies after making the first measurement, we performed the analysis by first slicing each membrane horizontally according to the molecular weight of proteins of interest. Each individual membrane strip was incubated with the primary anti-TRPC3, -TRPC6 and -GAPDH antibodies based on the known protein size and protein standard markers. The levels of TRPC proteins were normalized to loading control using the housekeeping protein GAPDH. Each strip from a single gel is shown as the example. Gels for each sample were run in triplicate and incubated with primary TRPC3, TRPC6 or glyceraldehyde 3-phosphate dehydrogenase followed by secondary fluorescent antibodies (Abcam, MA, USA). All antibody dilutions and signals were validated previously in our laboratory and by others[14,21]. Signals of the protein of interest were detected with Storm 860 fluorescent imaging system (GE Bio-Sciences, NJ, USA). Protein signals were quantified using MyImageAnalysis software (Thermo-Fisher Scientific, MA, USA) and the density of the TRPC proteins was normalized to the density of glyceraldehyde 3-phosphate dehydrogenase expression which is thought not to be differentially expressed in these models.

Statistics.-

No specific power calculation was conducted prior to experimentation, sample sizes used were based on our previous studies using other MH and non-MH animal models. Randomization methods were not used to assign the animals to be studied and blinding of the investigators was not used. All values are expressed as mean±SD, with n_{cells} representing the number of muscle fibers in which measurements were carried out and

N_{mice} representing the number of mice used either to isolate the fibers or for the *in vivo* experiments. Statistical analysis used two tailed hypothesis testing. For studies done on muscle fibers both *in vitro* and *in vivo* a one-way between subjects ANOVA was performed with Tukey's post-test for multiple measurements to determine significance ($p<0.05$). We used histograms (most commonly used graph to show frequency distributions) and the D'Agostino & Pearson test to assess the distribution of the data. Statistical analyses of western blots were carried out using an unpaired Student's independent T-test. To do this we used an independent samples T-Test, namely we compared two sample means from different populations regarding the same variable. The Mantel-Cox test was used to test for differences in survival between groups. All data collected was analyzed and no outliers were removed from our analyses. Statistical analysis was done using GraphPad Prism 7.03 (GraphPad Software, Inc.). Data from 11 mice were discarded due to: i) the loss of microelectrode sensitivity to calcium detected by a drift of more than 5 mV between the first and the second microelectrode calibration curves in the range between pCa6 - 7; ii) broken microelectrode tips which did not allow us to carry out the post measurement calibration curves; iii) the unexpected occurrence of electronic noise during the ion measurements that compromised the accuracy of the ion specific voltage recorded.

Results.-

Intracellular Ca^{2+} and Na^{+} concentrations in muscle fibers expressing a dominant negative TRPC6 channel.-

In vivo intracellular Ca^{2+} concentrations were 175% higher and intracellular Na^{+} concentrations were 88% higher in *RYR1*-p.R163C *vastus lateralis* muscle fibers than that observed in wild type muscle fibers ($p<0.0001$) (Figure 1). Expression of the dominant-negative TRPC6 reduced skeletal muscle intracellular Ca^{2+} and Na^{+} concentrations in both wild type and *RYR1*-p.R163C mice, however, the decreases caused by its expression were greater in *RYR1*-p.R163C/dominant negative TRPC6 than in wild type/dominant negative TRPC6 mice (43% ($p<0.0001$) *vs* 21% ($p<0.0001$), and 27% ($p<0.001$) *vs* 11% ($p=0.002$) for intracellular Ca^{2+} and Na^{+} concentrations respectively (Figure 1). There were no differences in resting membrane potential among the four different genotypes. Similar differences in intracellular Ca^{2+} and Na^{+} concentrations were observed *in-vitro* in enzymatically isolated single *flexor digitorum brevis* muscle fibers (Supplementary Figure 1).

Expressing a dominant negative TRPC6 channel in skeletal muscle reduces the elevation of intracellular Ca^{2+} and Na^{+} concentrations elicited by 1-oleoyl-2-acetyl-sn-glycerol.-

TRPC3/6 channels are directly activated by the ubiquitous intracellular second messenger diacylglycerol, whereas TRPC1/4/5 channels are not[22]. When we exposed single FDB muscle fibers to the membrane-permeable diacylglycerol analog 1-oleoyl-2-acetyl-sn-glycerol [22,21] (100μM) for 15 min intracellular Ca^{2+} concentration increased in *RYR1*-p.R163C fibers by 132% ($p<0.0001$), while in wild type fibers it increased by only

64% (p<0.0001) (Figure 2A). Similarly, 1-oleoyl-2-acetyl-sn-glycerol (100μM) produced a greater elevation of intracellular Na^+ concentration in *RYR1*-p.R163C *flexor digitorum brevis* muscle fibers (70%, p<0.0001) than in wild type (50%, p<0.0001) (Figure 2B). Similar results were obtained using 1,2-dioctanoyl-sn-glycerol, another membrane-permeable diacylglycerol analog[23] (Supplementary figure 2)**.** Expression of dominant negative TRPC6 reduced the effect of 1-oleoyl-2-acetyl-sn-glycerol on both intracellular Ca^{2+} and Na^+ concentrations in both wild type and *RYR1*-p.R163C *flexor digitorum brevis* muscle fibers. (Figure 2A and 2B).

Hyperforin induced elevation of resting intracellular Ca^{2+} concentration.-

To demonstrate that the changes in intracellular Ca^2 concentration seen with the expression of the dominant negative non-conducting TRPC6 transgene were due to a reduction in the function of TRPC6, we measured intracellular Ca^{2+} concentration in single muscle fibers exposed to the TRPC6 activator hyperforin[24]. We have previously found that hyperforin caused a genotype-dependent rise in resting intracellular Ca^{2+} concentration in the *RYR1*-p.G2435R murine MH model[14]. Here, we found that exposure of wild type and *RYR1*-p.R163C *flexor digitorum brevis* muscle fibers to 10 μM hyperforin produced a statistically significant increase in intracellular Ca^{2+} concentrations in both genotypes but the effect was less marked in wild type (34**%**, from 121±2nM to 162±15nM, p=<0.001) than in *RYR1*-p.R163C cells (54%, from 348±37nM to 537±70nM, p=<0.001) (Figure 3). Expression of dominant negative TRPC6 in *flexor digitorum brevis* muscle fibers markedly reduced the effect of hyperforin on intracellular Ca^{2+} concentration to only a 5% increase (from 94±6nM, to 99±6nM, p=0.248) in wild type/dominant negative

TRPC6 fibers and a 14% increase in *RYR1*-p.R163C/dominant negative TRPC6 fibers (from 185±11nM to 210±43nM p=0.288) (Figure 3).

Ethyl-1-(4-(2,3,3-trichloroacrylamide)phenyl)-5-(trifluoromethyl)-1H-pyrazole-4-carboxylate reduces intracellular Ca^{2+} concentration in RYR1-p.R163C/dominant negative TRPC6 skeletal muscle cells.-

The concept of functional specificity of Ca^{2+}-influx pathways was further explored by incubating single *flexor digitorum brevis* muscle fibers with the pyrazole compound ethyl-1-(4-(2,3,3-trichloroacrylamide)phenyl)-5-(trifluoromethyl)-1H-pyrazole-4-carboxylate, which is proposed to be a specific blocker of TRPC3[25]. Incubation with ethyl-1-(4-(2,3,3-trichloroacrylamide)phenyl)-5-(trifluoromethyl)-1H-pyrazole-4-carboxylate reduced intracellular Ca^{2+} concentration in *RYR1*-p.R163C *flexor digitorum brevis* muscle fibers from 352±29 to 268±34nM p<0.0001 and from 122±3nM to 108±7nM p<0.001 in wild type (Figure 4). Incubation with 10µM ethyl-1-(4-(2,3,3-trichloroacrylamide)phenyl)-5-(trifluoromethyl)-1H-pyrazole-4-carboxylate almost normalized intracellular Ca^{2+} concentration in *RYR1*-p.R163C/dominant negative TRPC6 fibers from 190±15nM to 130±9nM p<0.0001 and reduced intracellular Ca^{2+} concentration in wild type/dominant negative TRPC6 fibers from 93±9nM to 79±8nM p<0.001 (Figure 4). In both wild type and *RYR1*-p.R163C/dominant negative TRPC6 genotypes, the percent reduction caused by ethyl-1-(4-(2,3,3-trichloroacrylamide)phenyl)-5-(trifluoromethyl)-1H-pyrazole-4-carboxylate was similar to the percent reduction seen after ethyl-1-(4-(2,3,3-trichloroacrylamide)phenyl)-5-(trifluoromethyl)-1H-pyrazole-4-carboxylate exposure in the absence of dominant negative TRPC6 expression.

Expression of dominant negative TRPC6 reduced the increase of intracellular Ca^{2+} concentration in RYR1-p.R163C muscle during exposure to halothane.-

Exposure to 2% halothane had no effect on intracellular Ca^{2+} concentration measured *in vivo* in the *vastus lateralis* fibers of wild type mice but caused an immediate and statistically significant 273% elevation in intracellular Ca^{2+} concentration ($p<0.0001$) in the *vastus lateralis* fibers of *RYR1*-p.R163C mice (Figure 5). Furthermore, all the *RYR1*-p.R163C animals succumbed to the MH crisis within 16 min of halothane exposure (Figure 6). Expression of dominant negative TRPC6 in *RYR1*-p.R163C muscle, in addition to reducing intracellular Ca^{2+} concentration (Figure 5) before exposure to halothane, both statistically significantly attenuated the increase in intracellular Ca^{2+} concentration (125% vs 275%, $p<0.0001$) during exposure to halothane (Figure 5) and statistically significantly increased the survival time (Figure 6). The mean survival time of *RYR1*-p.R163C/dominant negative TRPC6 mice was 35±5 min ($N_{mice}=7$) *vs* 15±3 min for *RYR1*-p.R163C mice ($N_{mice}=7$) ($p<0.0001$). However, dominant negative TRPC6 expression was not sufficient to entirely prevent the elevation of intracellular Ca^{2+} concentration after halothane inhalation over time and did not prevent death as a result of the MH crisis. Figure 7 shows an experiment in which intracellular Ca^{2+} concentration and rectal temperature were recorded continuously *in vivo* in a *RYR1*-p.R163C/dominant negative TRPC6 mouse until it succumbed to the MH crisis. Intracellular Ca^{2+} concentration rapidly increased from 236 nM to 465 nM immediately after exposure to halothane and remained between 422-498 nM for the next 14-18 min, and then increased slowly reaching 900-1000 nM after 34 min of halothane inhalation when death occurred.

Effects of ethyl-1-(4-(2,3,3-trichloroacrylamide)phenyl)-5-(trifluoromethyl)-1H-pyrazole-4-carboxylate in RYR1-p.R163C/*dominant negative TRPC6 *muscles during exposure to halothane.-

Although it was not possible to administer ethyl-1-(4-(2,3,3-trichloroacrylamide)phenyl)-5-(trifluoromethyl)-1H-pyrazole-4-carboxylate systemically, we were able to measure its local effects on skeletal muscle intracellular Ca^{2+} concentration *in vivo* by measuring intracellular Ca^{2+} concentration simultaneously in the left and right *vastus lateralis* muscles in wild type/dominant negative TRPC6 and *RYR1*-p.R163C/dominant negative TRPC6 mice before and after exposure to 2% halothane. The left leg muscle was used as a control while the right leg muscle was superfused continuously with 10 µM ethyl-1-(4-(2,3,3-trichloroacrylamide)phenyl)-5-(trifluoromethyl)-1H-pyrazole-4-carboxylate for 15 min prior to and during the entire exposure to halothane. In the wild type/dominant negative TRPC6-left leg muscle the intracellular Ca^{2+} concentration was 95±4nM and this was unchanged after exposure to halothane (93±5nM) (Figure 8A). Intracellular Ca^{2+} concentration was reduced to 84±6nM after 15 min of local incubation with 10 µM ethyl-1-(4-(2,3,3-trichloroacrylamide)phenyl)-5-(trifluoromethyl)-1H-pyrazole-4-carboxylate and as before was unaffected by exposure to 2% halothane (86±6.2nM) (Figure 8A). In *RYR1*-p.R163C/dominant negative TRPC6 muscle basal intracellular Ca^{2+} concentration was 186±20nM and rose to 415±29nM immediately after exposure to 2% halothane (Figure 8B). Incubation with ethyl-1-(4-(2,3,3-trichloroacrylamide)phenyl)-5-(trifluoromethyl)-1H-pyrazole-4-carboxylate reduced basal intracellular Ca^{2+} concentration from 194±11nM to 146±12nM (p<0.0001) and statistically significantly blunted the increase seen after exposure to halothane

(250±27nM (p<0.0001)) compared to the untreated *RYR1*-p.R163C/dominant negative TRPC6-left leg muscle (Figure 8B).

Measurements of TRPC3 and TRPC6 expression in muscle cells.-

We determined the expression of TRPC 3 and TRPC 6 channels in *Gastrocnemius* muscle homogenates from wild type, wild type/dominant negative TRPC6, *RYR1*-p.R163C and *RYR1*-p.R163C/dominant negative TRPC6 mice. As expected from our previous studies on murine models relevant to MH[14] western blot analysis demonstrated a statistically significantly increased expression of both TRPC3 and TRPC6 proteins in *RYR1*-p.R163C compared to wild type muscles (p<0.0001 and p<0.0001 respectively). Furthermore, as expected we were able to see a statistically significant increase in TRPC6 expression in wild type/dominant negative TRPC6, and *RYR1*-p.R163C/dominant negative TRPC6 muscles compared to controls (p=0.002 and p=0.008 respectively). Unexpectedly we observed that concomitantly with the expected transgenic overexpression of TRPC6 there was a statistically significant increase in the expression of TRPC3 protein in both wild type/dominant negative TRPC6 (p=0.013) compared to Wt (p=0.002)and *RYR1*-p.R163C/dominant negative TRPC6 compared to *RYR1*-p.R163C muscles (p=0.014). Figure 9A shows a representative western blot from the 4 genotypes and quantification graphs reflecting relative expression levels of TRPC3 and TRPC6 proteins normalized to the expression of glyceraldehyde 3-phosphate dehydrogenase (Figure 9B).

Discussion.-

We have demonstrated that muscle-specific overexpression of the non-conducting TRPC6 channel both reduced intracellular Ca^{2+} concentration in *RYR1*-p.R163C animals at rest and reduced the absolute maximum levels of intracellular Ca^{2+} concentration reached during exposure to halothane. Despite this, its expression did not restore intracellular Ca^{2+} concentration to wild type levels and although its expression increased the length of survival after the exposure to halothane it was unable to rescue the lethal phenotype. The physiologic effect of muscle-specific expression of a dominant negative TRPC6 on TRPC6 function was confirmed by the marked attenuation of reactivity of expressing muscle fibers to the TRPC6 activator hyperforin. Although there was a compensatory increase in expression of TRPC3 in dominant negative TRPC6 mice, this does not explain the failure of molecular inhibition of TRPC6 channels to fully restore responses in *RYR1*-p.R163C animals and fibers to that of wild type because the addition of ethyl-1-(4-(2,3,3-trichloroacrylamide)phenyl)-5-(trifluoromethyl)-1H-pyrazole-4-carboxylate, a TRPC3 blocker, still resulted in elevated intracellular Ca^{2+} concentrations at rest and during exposure to halothane. Indeed, the contribution of TRPC3 to intracellular Ca^{2+} concentration was proportionally similar in *RYR1*-p.R163C fibers in the presence or absence of dominant negative TRPC6. Our findings of an effect of dominant negative TRPC6 and ethyl-1-(4-(2,3,3-trichloroacrylamide)phenyl)-5-(trifluoromethyl)-1H-pyrazole-4-carboxylate in wild type fibers demonstrate that TRPC3/6 channels contribute to physiologic levels of intracellular Ca^{2+} concentration in skeletal muscle. It is possible that their role is to help maintain intracellular Ca^{2+} store content during muscle activity

and this effect could be mediated through diacylglycerol signaling in response to elevations in intracellular Ca^{2+} concentration.

Molecular genetic studies have established the type 1 ryanodine receptor (*RYR1*) gene encoding the skeletal muscle sarcoplasmic reticulum Ca^{2+} release channel as the primary locus for MH susceptibility[2,4,5] and secondary loci have been identified in other proteins involved with RyR1 in excitation-contraction coupling[26,27] that are thought to sensitize the RyR1 channel. A common characteristic of muscle expressing MH-RyR1 variants is an increased intracellular Ca^{2+} concentration that is thought to be caused by increased RyR1 leak[8,9,11,19,28,29]. However, evidence accumulated over the past decade suggest more complex molecular mechanisms by which a sensitized RyR1 channel results in a MH reaction upon exposure to triggering anesthetics, as well as non-anesthetic phenotypes associated with MH susceptibility.

The importance of extracellular Ca^{2+} to the effects of halothane in MH susceptible muscle was suggested more than 40 years ago[30]. More recently, Duke et al.[31], Eltit et al.[13], and Lopez et al.[14], have demonstrated trans-sarcolemmal Ca^{2+} influx in human and mouse MH muscle which appears to be mediated by store-operated Ca^{2+} entry, canonical transient receptor potential channels, or both. The present study both confirms augmented expression of TRPC3 and TRPC6 in MH muscle fibers[13,14] and unequivocally demonstrates, through specific molecular inhibition, the contribution of TRPC channels that is predominantly mediated through TRPC6. Indeed, the intracellular Ca^{2+} dyshomeostasis observed in MH susceptible muscle could not be sustained solely by sarcoplasmic reticulum Ca^{2+} leak/release, but instead a combination of this and TRPC-

mediated trans-sarcolemmal Ca^{2+} influx were required with the latter being the major player in terms of Ca^{2+} contribution.

TRPC channels constitute a large and functionally versatile superfamily of cation channel proteins expressed in many cell types and which control influxes of Ca^{2+} and other cations (sodium, lithium and magnesium)[32] to regulate diverse cellular processes . In skeletal muscle, they seem to be involved in muscle development, store-operated entry of Ca^{2+}, response to stretch[33], and modulation of glucose transport[34]. TRPC channels are activated by diacylglycerol generated in response to phospholipase C-induced phosphatidylinositol 4,5 bisphosphate hydrolysis[22]. A driving force behind the recent research in the field of TRPCs in muscle is the idea that TRPCs could be involved through abnormal Ca^{2+} signaling in several striated muscle pathologies, such as Duchenne muscular dystrophy[33,35,36], myocardial remodeling and hypertrophy[34] and malignant hyperthermia[13,14].

Defining the large but still partial contributions of TRPC3 and 6 to elevated intracellular Ca^{2+} concentration in MH susceptible muscle at rest and during a MH episode draws attention to other contributing mechanisms. It is possible that sarcoplasmic reticulum Ca^{2+} leak could fully explain residual increases in intracellular Ca^{2+} concentration but it is the responses to halothane we find especially intriguing. We have previously reported that the reverse mode function of the sodium-calcium exchanger contributes to the elevation of intracellular Ca^{2+} during the MH episode[18], and this may also explain the findings in the muscle of *RYR1*-p.R163C/dominant negative TRPC6 mice pretreated with the TRPC3 inhibitor ethyl-1-(4-(2,3,3-trichloroacrylamide)phenyl)-5-(trifluoromethyl)-1H-pyrazole-4-carboxylate before addition of halothane. The reverse

mode sodium-calcium exchanger can be activated following localized intracellular Na^+ accumulation through non-selective TRPC[13,14] and SOC channels. Furthermore, NCX has also been demonstrated to interact both physically and functionally with certain TRPC channels and evidence has been presented for the link between STIM1 mediated Na^+ influx and the activation of NCX[37]. Here there was an initial, relatively small, increase in intracellular Ca^{2+} concentration to a level that was sustained for approximately 10 minutes before the beginning of a second slower more marked and progressive increase which paralleled the increase in the rectal temperature of the animal. Such a pattern suggests that the initial plateau represents a new equilibrium where increased calcium sequestration compensates for increased sarcoplasmic reticulum calcium release. Clearly this status quo cannot be sustained. Decompensation might occur if there is disruption of ATP production, which could occur with excessive mitochondrial uptake of calcium, leading to reduced calcium sequestration capacity. Alternatively, mitochondrial dysfunction secondary to calcium uptake could result in increased production of reactive oxygen species that can result in increased *RYR1*-mediated calcium release[38,39]. A further possibility is that the sarcoplasmic reticulum calcium content decreases during the plateau phase to reach the level at which store-operated calcium entry is initiated leading to a massive sustained influx of extracellular calcium[31].

This study is not without limitations. The main limitation of this work is that it is conducted using mice and mouse tissue rather than humans and human tissue. Although murine models relevant to malignant hyperthermia appear more sensitive to environmental heat stress than malignant hyperthermia susceptible patients, they recapitulate the human condition in many other respects, including increased intracellular

Ca^{2+} concentration[9,28,40], dependence on extracellular calcium[31], and mitochondrial dysfunction[41]. We have also not demonstrated that skeletal muscle specific expression of a non-conducting dominant negative TRPC6 completely abolishes TRPC6 conductance, although previous work with this construct suggests this is likely[15].

Finally, while we have used molecular inhibition of TRPC6, our conclusions concerning the effect of ethyl-1-(4-(2,3,3-trichloroacrylamide)phenyl)-5-(trifluoromethyl)-1H-pyrazole-4-carboxylate on TRPC3 must be more guarded as selectivity of pharmacologic reagents can never be guaranteed.

In summary, these results demonstrate that nonselective sarcolemmal cation permeability mediated by TRPC6 and TRPC3 plays a critical role in causing cytosolic Ca^{2+} overload both at rest and during a malignant hyperthermia crisis. This improved understanding of the underlying mechanisms of malignant hyperthermia may assist in the design of new therapies and the identification of more selective pharmacological agents other than our current gold standard, dantrolene, to prevent or reverse the malignant hyperthermia episodes.

Acknowledgments.

We are grateful to Dr. James D Molkentin for generously providing us with the transgenic mice with skeletal muscle-specific overexpression of a non-conducting TRPC6 channel and Shane Antrobus for his valuable technical assistance.

References.-

1. Rosenberg H, Pollock N, Schiemann A, Bulger T, Stowell K: Malignant hyperthermia: a review. Orphanet J Rare Dis 2015; 10: 93
2. MacLennan DH, Duff C, Zorzato F, Fujii J, Phillips M, Korneluk RG, Frodis W, Britt BA, Worton RG: Ryanodine receptor gene is a candidate for predisposition to malignant hyperthermia. Nature 1990; 343: 559-61
3. Kausch K, Lehmann-Horn F, Janka M, Wieringa B, Grimm T, Muller CR: Evidence for linkage of the central core disease locus to the proximal long arm of human chromosome 19. Genomics 1991; 10: 765-9
4. Robinson R, Carpenter D, Shaw MA, Halsall J, Hopkins P: Mutations in RYR1 in malignant hyperthermia and central core disease. Hum Mutat 2006; 27: 977-89
5. Jurkat-Rott K, McCarthy T, Lehmann-Horn F: Genetics and pathogenesis of malignant hyperthermia. Muscle Nerve 2000; 23: 4-17
6. Miller DM, Daly C, Aboelsaod EM, Gardner L, Hobson SJ, Riasat K, Shepherd S, Robinson RL, Bilmen JG, Gupta PK, Shaw MA, Hopkins PM: Genetic epidemiology of malignant hyperthermia in the UK. Br J Anaesth 2018; 121: 944-952
7. Lopez JR, Alamo L, Caputo C, Wikinski J, Ledezma D: Intracellular ionized calcium concentration in muscles from humans with malignant hyperthermia. Muscle Nerve 1985; 8: 355-8
8. Lopez JR, Alamo LA, Jones DE, Papp L, Allen PD, Gergely J, Sreter FA: [Ca2+]i in muscles of malignant hyperthermia susceptible pigs determined in vivo with Ca2+ selective microelectrodes. Muscle Nerve 1986; 9: 85-6
9. Yang T, Esteve E, Pessah IN, Molinski TF, Allen PD, Lopez JR: Elevated resting [Ca(2+)](i) in myotubes expressing malignant hyperthermia RyR1 cDNAs is partially restored by modulation of passive calcium leak from the SR. Am J Physiol Cell Physiol 2007; 292: C1591-8
10. Eltit JM, Bannister RA, Moua O, Altamirano F, Hopkins PM, Pessah IN, Molinski TF, Lopez JR, Beam KG, Allen PD: Malignant hyperthermia susceptibility arising from altered resting coupling between the skeletal muscle L-type Ca2+ channel and the type 1 ryanodine receptor. Proc Natl Acad Sci U S A 2012; 109: 7923-8
11. Lopez JR, Allen PD, Alamo L, Jones D, Sreter FA: Myoplasmic free [Ca2+] during a malignant hyperthermia episode in swine. Muscle Nerve 1988; 11: 82-8
12. Yuen B, Boncompagni S, Feng W, Yang T, Lopez JR, Matthaei KI, Goth SR, Protasi F, Franzini-Armstrong C, Allen PD, Pessah IN: Mice expressing T4826I-RYR1 are viable but exhibit sex- and genotype-dependent susceptibility to malignant hyperthermia and muscle damage. FASEB J 2012; 26: 1311-22
13. Eltit JM, Ding X, Pessah IN, Allen PD, Lopez JR: Nonspecific sarcolemmal cation channels are critical for the pathogenesis of malignant hyperthermia. FASEB J 2013; 27: 991-1000
14. Lopez JR KV, Hopkins P, Uryach A, Adams J, Allen PD: The role of transient receptor potential cation channels in calcium dyshomeostasis in
a mouse model relevant to Malignant Hyperthermia. Anesthesiology 2020; In Press
15. Millay DP, Goonasekera SA, Sargent MA, Maillet M, Aronow BJ, Molkentin JD: Calcium influx is sufficient to induce muscular dystrophy through a TRPC-dependent mechanism. Proc Natl Acad Sci U S A 2009; 106: 19023-8

16. Hofmann T, Schaefer M, Schultz G, Gudermann T: Subunit composition of mammalian transient receptor potential channels in living cells. Proc Natl Acad Sci U S A 2002; 99: 7461-6
17. Tang Q, Guo W, Zheng L, Wu JX, Liu M, Zhou X, Zhang X, Chen L: Structure of the receptor-activated human TRPC6 and TRPC3 ion channels. Cell Res 2018; 28: 746-755
18. Altamirano F, Eltit JM, Robin G, Linares N, Ding X, Pessah IN, Allen PD, Lopez JR: Ca2+ influx via the Na+/Ca2+ exchanger is enhanced in malignant hyperthermia skeletal muscle. J Biol Chem 2014; 289: 19180-90
19. Lopez JR, Alamo L, Caputo C, DiPolo R, Vergara S: Determination of ionic calcium in frog skeletal muscle fibers. Biophys J 1983; 43: 1-4
20. Altamirano F, Perez CF, Liu M, Widrick J, Barton ER, Allen PD, Adams JA, Lopez JR: Whole body periodic acceleration is an effective therapy to ameliorate muscular dystrophy in mdx mice. PLoS One 2014; 9: e106590
21. Laemmli UK: Cleavage of structural proteins during the assembly of the head of bacteriophage T4. Nature 1970; 227: 680-5
22. Hofmann T, Obukhov AG, Schaefer M, Harteneck C, Gudermann T, Schultz G: Direct activation of human TRPC6 and TRPC3 channels by diacylglycerol. Nature 1999; 397: 259-63
23. Aires V, Hichami A, Boulay G, Khan NA: Activation of TRPC6 calcium channels by diacylglycerol (DAG)-containing arachidonic acid: a comparative study with DAG-containing docosahexaenoic acid. Biochimie 2007; 89: 926-37
24. Leuner K, Kazanski V, Muller M, Essin K, Henke B, Gollasch M, Harteneck C, Muller WE: Hyperforin--a key constituent of St. John's wort specifically activates TRPC6 channels. FASEB J 2007; 21: 4101-11
25. Kiyonaka S, Kato K, Nishida M, Mio K, Numaga T, Sawaguchi Y, Yoshida T, Wakamori M, Mori E, Numata T, Ishii M, Takemoto H, Ojida A, Watanabe K, Uemura A, Kurose H, Morii T, Kobayashi T, Sato Y, Sato C, Hamachi I, Mori Y: Selective and direct inhibition of TRPC3 channels underlies biological activities of a pyrazole compound. Proc Natl Acad Sci U S A 2009; 106: 5400-5
26. Robinson RL, Monnier N, Wolz W, Jung M, Reis A, Nuernberg G, Curran JL, Monsieurs K, Stieglitz P, Heytens L, Fricker R, van Broeckhoven C, Deufel T, Hopkins PM, Lunardi J, Mueller CR: A genome wide search for susceptibility loci in three European malignant hyperthermia pedigrees. Hum Mol Genet 1997; 6: 953-61
27. Stamm DS, Powell CM, Stajich JM, Zismann VL, Stephan DA, Chesnut B, Aylsworth AS, Kahler SG, Deak KL, Gilbert JR, Speer MC: Novel congenital myopathy locus identified in Native American Indians at 12q13.13-14.1. Neurology 2008; 71: 1764-9
28. Yang T, Riehl J, Esteve E, Matthaei KI, Goth S, Allen PD, Pessah IN, Lopez JR: Pharmacologic and functional characterization of malignant hyperthermia in the R163C RyR1 knock-in mouse. Anesthesiology 2006; 105: 1164-75
29. Lopez JR, Kaura V, Diggle CP, Hopkins PM, Allen PD: Malignant hyperthermia, environmental heat stress, and intracellular calcium dysregulation in a mouse model expressing the p.G2435R variant of RYR1. Br J Anaesth 2018; 121: 953-961

30. Nelson TE, Bedell DM, Jones EW: Porcine malignant hyperthermia: effects of temperature and extracellular calcium concentration on halothane-induced contracture of susceptible skeletal muscle. Anesthesiology 1975; 42: 301-6
31. Duke AM, Hopkins PM, Calaghan SC, Halsall JP, Steele DS: Store-operated Ca2+ entry in malignant hyperthermia-susceptible human skeletal muscle. J Biol Chem 2010; 285: 25645-53
32. Owsianik G, Talavera K, Voets T, Nilius B: Permeation and selectivity of TRP channels. Annu Rev Physiol 2006; 68: 685-717
33. Lopez JR, Uryash A, Faury G, Esteve E, Adams JA: Contribution of TRPC Channels to Intracellular Ca(2 +) Dyshomeostasis in Smooth Muscle From mdx Mice. Front Physiol 2020; 11: 126
34. Eder P: Cardiac Remodeling and Disease: SOCE and TRPC Signaling in Cardiac Pathology. Adv Exp Med Biol 2017; 993: 505-521
35. Mijares A, Altamirano F, Kolster J, Adams JA, Lopez JR: Age-dependent changes in diastolic Ca(2+) and Na(+) concentrations in dystrophic cardiomyopathy: Role of Ca(2+) entry and IP3. Biochem Biophys Res Commun 2014; 452: 1054-9
36. Matsumura CY, Taniguti AP, Pertille A, Santo Neto H, Marques MJ: Stretch-activated calcium channel protein TRPC1 is correlated with the different degrees of the dystrophic phenotype in mdx mice. Am J Physiol Cell Physiol 2011; 301: C1344-50
37. Liu B, Peel SE, Fox J, Hall IP: Reverse mode Na+/Ca2+ exchange mediated by STIM1 contributes to Ca2+ influx in airway smooth muscle following agonist stimulation. Respir Res 2010; 11: 168
38. Dridi H, Yehya M, Barsotti R, Reiken S, Angebault C, Jung B, Jaber S, Marks AR, Lacampagne A, Matecki S: Mitochondrial oxidative stress induces leaky ryanodine receptor during mechanical ventilation. Free Radic Biol Med 2020; 146: 383-391
39. Lotteau S, Ivarsson N, Yang Z, Restagno D, Colyer J, Hopkins P, Weightman A, Himori K, Yamada T, Bruton J, Steele D, Westerblad H, Calaghan S: A Mechanism for Statin-Induced Susceptibility to Myopathy. JACC Basic Transl Sci 2019; 4: 509-523
40. Yang T, Allen PD, Pessah IN, Lopez JR: Enhanced excitation-coupled calcium entry in myotubes is associated with expression of RyR1 malignant hyperthermia mutations. J Biol Chem 2007; 282: 37471-8
41. Chang L, Daly C, Miller DM, Allen PD, Boyle JP, Hopkins PM, Shaw MA: Permeabilised skeletal muscle reveals mitochondrial deficiency in malignant hyperthermia-susceptible individuals. Br J Anaesth 2019; 122: 613-621

Figure Legends

Figure 1. ***Reduced intracellular Ca^{2+} and Na^{+} concentrations in muscle fibers expressing a dominant negative TRPC6 channel***. Intracellular Ca^{2+} or Na^{+} concentration was measured on the superficial *vastus lateralis* muscle fibers -*in vivo*- in wild type, wild type/dominant negative TRPC6, *RYR1*-p.R163C and *RYR1*-p.R163C/dominant negative TRPC6 mice using double-barreled ion-specific microelectrodes. N_{mice}=7/genotype, Wild Type, n_{cells}=35; Wild Type dominant negative TRPC6, n_{cells}=34; *RYR1*-p.R163C n_{cells}=25; *RYR1*-p.R163C/dominant n_{cells}=35 for intracellular Ca^{2+} concentration measurements. For intracellular Na^{+} concentration measurements, N_{mice}=4/genotype Wild Type, n_{cells}=20; Wild Type dominant negative TRPC6, n_{cells}=15; *RYR1*-p.R163C, n_{cells}=15; *RYR1*-p.R163C/dominant negative TRPC6,, n_{cells}=15. Values are expressed as means±S.D. for each condition. Statistical analysis was done using a one-way ANOVA with Tukey's post-test, *$p \leq 0.05$.

Figure 2. ***Expressing a dominant negative TRPC6 channel reduces the elevation of intracellular Ca^{2+} and Na^{+} concentrations elicited by 1-oleoyl-2-acetyl-sn-glycerol.*** Exposure of quiescent *flexor digitorium brevis* muscle fibers isolated from wild type, wild type/dominant negative TRPC6, *RYR1*-p.R163C and *RYR1*-p.R163C /dominant negative TRPC6 mice to 100µM 1-oleoyl-2-acetyl-sn-glycerol induced an elevation of intracellular Ca^{2+} (**Fig. 2A**) and Na^{+} concentration (**Fig. 2B**). Expression of dominant negative TRPC6 reduced the effect of 1-oleoyl-2-acetyl-sn-glycerol on both intracellular Ca^{2+} (**Fig. 2A**) and Na^{+} (**Fig. 2B**) concentrations in both wild type and *RYR1*-p.R163C muscle fibers. The experimental conditions are indicated on the horizontal axis. For intracellular Ca^{2+} concentration measurements: N_{mice}=5/genotype, Wild Type, n_{cells}=25; Wild Type dominant negative TRPC6, n_{cells}=20; *RYR1*-p.R163C n_{cells}=20; *RYR1*-p.R163C/dominant n=21 for intracellular Ca^{2+} concentration measurements. For intracellular Na^{+} concentration measurements: N_{mice}=3/genotype. Wild Type, n_{cells}=15; Wild Type dominant negative TRPC6, n_{cells}=17; *RYR1*-p.R163C n_{cells}=18; *RYR1*-p.R163C/ dominant negative TRPC6 n_{cells}=15. Values are expressed as means±S.D. for each condition. Statistical analysis was done using a one-way ANOVA with Tukey's post-test, *$p \leq 0.05$.

Figure 3. ***Hyperforin induced an elevation of intracellular Ca^{2+} concentration.*** Incubation of *flexor digitorium brevis* muscle fibers isolated from wild type, wild type/dominant negative TRPC6, *RYR1*-p.R163C and *RYR1*-p.R163C /dominant negative TRPC6 mice with 10µM hyperforin produced a statistically significant ($p<0.0001$) increase in intracellular Ca^{2+} concentration in all genotypes but the effect was more marked in *RYR1*-p.R163C fibers than in wild type. Expression of dominant negative TRPC6 in wild type and *RYR1*-p.R163C reduced the effect of hyperforin. The experimental conditions used are indicated on the horizontal axis. For intracellular Ca^{2+} concentration measurements: N_{mice}=5/genotype, Wild Type, n_{cells}=19; Wild Type dominant negative TRPC6, n_{cells}=20; *RYR1*-p.R163C n_{cells}=22; *RYR1*-p.R163C/ dominant negative TRPC6 n_{cells}=20. Values are expressed as means±S.D. for each condition. Statistical analysis was done using a one-way ANOVA with Tukey's post-test, *$p \leq 0.05$.

Figure 4*. Effect of ethyl-1-(4-(2,3,3-trichloroacrylamide)phenyl)-5-(trifluoromethyl)-1H-pyrazole-4-carboxylate on intracellular Ca^{2+} and Na^{+}*. 10μM Ethyl-1-(4-(2,3,3-trichloro-acrylamide)phenyl)-5-(trifluoromethyl)-1H-pyrazole-4-carboxylate reduced intracellular Ca^{2+} concentration in the *flexor digitorium brevis* muscles of all genotype's. The experimental conditions used are indicated on the horizontal axis. For intracellular Ca^{2+} determinations: N_{mice}=5/genotype, Wild Type, n_{cells}=20; Wild Type - Ethyl-1-(4-(2,3,3-trichloro-acrylamide)phenyl)-5-(trifluoromethyl)-1H-pyrazole-4-carboxylate, n_{cells}=23; Wild Type dominant negative TRPC6, n_{cells}=19; Wild Type dominant negative TRPC6-Ethyl-1-(4-(2,3,3-trichloro-acrylamide)phenyl)-5-(trifluoromethyl)-1H-pyrazole-4-carboxylate n_{cells}=21; *RYR1*-p.R163C n_{cells}=22; *RYR1*-p.R163C-Ethyl-1-(4-(2,3,3-trichloro-acrylamide)phenyl)-5-(trifluoromethyl)-1H-pyrazole-4-carboxylate n_{cells}=21; *RYR1*-p.R163C dominant negative TRPC6 n_{cells}=20; *RYR1*-p.R163C dominant negative TRPC6-Ethyl-1-(4-(2,3,3-trichloro-acrylamide)phenyl)-5-(trifluoromethyl)-1H-pyrazole-4-carboxylate n_{cells}=22. Values are expressed as means±S.D. for each condition. Statistical analysis was done using a one-way ANOVA with Tukey's post-test, $*p \leq 0.05$.

Figure 5. *Expression of dominant negative TRPC6 reduced the increase of intracellular Ca^{2+} concentration in RYR1-p.R163C muscle during exposure to halothane.* Intracellular Ca^{2+} concentration was measured *in vivo* in the *vastus lateralis* fibers of wild type, wild type/dominant negative TRPC6, *RYR1*-p.R163C, and *RYR1*-p.R163C dominant/negative TRPC6 before and after the inhalation of 2% halothane. In wild type muscle fibers, halothane did not provoke elevation in intracellular Ca^{2+} concentration, while in *RYR1*-p.R163C induced a robust an immediate elevation of intracellular Ca^{2+} concentration***.*** Expression of dominant negative TRPC6 in *RYR1*-p.R163C muscle, reduced intracellular Ca^{2+} concentration, and statistically significantly attenuated the increase in intracellular Ca^{2+} concentration during inhalation of halothane. The experimental conditions used are indicated on the horizontal axis. For intracellular Ca^{2+} concentration measurements in N_{mice}=7/genotype, Wild Type, n_{cells}=35; Wild Type dominant negative TRPC6, n_{cells}=32; *RYR1*-p.R163C n_{cells}=23; *RYR1*-p.R163C/dominant negative TRPC6 n_{cells}=37. Values are expressed as means±S.D. for each condition. Statistical analysis was done using a one-way ANOVA with Tukey's post-test, $*p \leq 0.05$.

Figure 6. *The survival of R163C mice is enhanced by* expression. Kaplan-Meier survival curves reveal that expression of dominant TRPC6 statistically significantly increased the mice survival time in *RYR1*-p.R163C mice from 15.3±3 min to 35.5±5 min *RYR1*-p.R163C/dominant negative TRPC6. N_{mice}=7/genotype. Values are expressed as means ± S.D. for each condition. Statistical analysis was done using a one-way ANOVA with Tukey's post-test, $*p \leq 0.05$.

Figure 7. *Time course of changes in intracellular Ca^{2+} and rectal temperature in a mouse expressing dominant negative TRPC6.* A typical experiment carried out *in vivo* in an anesthetized (ketamine/xylazine) *RYR1*-p.R163C/dominant negative TRPC6 mouse. Intracellular calcium concentration on the superficial fibers of the *vastus lateralis* muscle and rectal temperature were measured simultaneously before and after halothane

2% inhalation. The insert on the left upper corner shows the time of death after halothane inhalation.

Figure 8. *Ethyl-1-(4-(2,3,3-trichloroacrylamide)phenyl)-5-(trifluoromethyl)-1H-pyrazole-4-carboxylate reduces intracellular Ca^{2+} concentration in* RYR1-p.R163C/dominant negative TRPC6 *skeletal muscle cells.* Intracellular Ca^{2+} concentration was measured in both the right and left *vastus lateralis* muscle of **(A)** wild type/dominant negative TRPC6 and **(B)** *RYR1*-p.R163C/dominant negative TRPC6 muscles. In both the right leg was superfused with the TRPC3 blocker Ethyl-1-(4-(2,3,3-trichloroacrylamide)phenyl)-5-(trifluoromethyl)-1H-pyrazole-4-carboxylate, and Ca^{2+} was measured a second time, after which the animal was exposed to 2% halothane and Intracellular Ca^{2+} concentration was measured in both the right and left *vastus lateralis* muscle a final time. N_{mice}=5/genotype, Wild Type dominant negative TRPC6 (LL), n_{cells}=20; Wild Type dominant negative TRPC6 (LL) - Halothane, n_{cells}=18; Wild Type dominant negative TRPC6 (RL), n_{cells} =17; Wild Type dominant negative TRPC6 (RL) Ethyl-1-(4-(2,3,3-trichloroacrylamide)phenyl)-5-(trifluoromethyl)-1H-pyrazole-4-carboxylate, n_{cells}=20; Wild Type dominant negative TRPC6 (RL), Ethyl-1-(4-(2,3,3-trichloroacrylamide)phenyl)-5-(trifluoromethyl)-1H-pyrazole-4-carboxylate and halothane, n_{cells}=19. *RYR1*-p.R163C/ dominant negative TRPC6 (LL) n=22; *RYR1*-p.R163C/ dominant negative TRPC6 (LL) – Halothane, n_{cells}=22; *RYR1*-p.R163C/ dominant negative TRPC6 (RL), n_{cells}=21; *RYR1*-p.R163C/ dominant negative TRPC6 (RL) Ethyl-1-(4-(2,3,3-trichloroacrylamide)phenyl)-5-(trifluoromethyl)-1H-pyrazole-4-carboxylate and halothane, n_{cells}=21; *RYR1*-p.R163C/ dominant negative TRPC6 (RL) Ethyl-1-(4-(2,3,3-trichloroacrylamide)phenyl)-5-(trifluoromethyl)-1H-pyrazole-4-carboxylate and halothane n_{cells}=22. The experimental conditions used are indicated on the horizontal axis. Values are expressed as means±S.D. for each condition. Statistical analysis was done using a one-way ANOVA with Tukey's post-test, *$p \leq 0.05$.

Figure 9. *Measurements of TRPC3 and TRPC6 protein expression in gastrocnemius muscles*. (**A)** A representative Western blot analysis of the expression of TRPC3, TRPC6, and glyceraldehyde 3-phosphate dehydrogenase in *gastrocnemius* muscle from wild type, wild type/dominant negative TRPC6, *RYR1*-p.R163C and *RYR1*-p.R163C /dominant negative TRPC6 mice. **(B)** Shows the summary of the densitometric analysis. Data were normalized to glyceraldehyde 3-phosphate dehydrogenase and expressed as mean optical unit values ± S.D. N_{mice}=3/genotype. For the TRPC3 and TRPC 6 proteins expression, the densitometric quantitative data was based in 3 independent experiments from each mouse . Values are expressed as means±S.D. for each condition. Statistical analysis was done using unpaired Student's independent *t*-test, *$p \leq 0.05$.

Supplementary Figure 1. *Expression of dominant negative TRPC6 channels reduced intracellular Ca^{2+} and Na^{+} in isolated muscle fibers.* Intracellular calcium or sodium concentrations were measured in quiescent isolated *flexor digitorium brevis* muscle fibers from wild type, wild type/dominant negative TRPC6, *RYR1*-p.R163C and *RYR1*-p.R163C /dominant negative TRPC6 mice using double-barreled ion-specific microelectrodes. Intracellular calcium and sodium were statistically significantly (p<0.0001) higher in *RYR1*-p.R163C than wild type. Expression of dominant negative

TRPC6 reduced Intracellular calcium and sodium in all genotypes. For intracellular Ca^{2+} concentration measurements N_{mice}=3/genotype, Wild Type, n_{cells}=14; Wild Type dominant negative TRPC6, n=13; *RYR1*-p.R163C n_{cells}=16; *RYR1*-p.R163C/ dominant negative TRPC6 n_{cells}=15. For intracellular Na^+ concentration measurements N_{mice}=3/genotype, Wild Type, n_{cells}=13; Wild Type dominant negative TRPC6, n_{cells}=12; *RYR1*-p.R163C n_{cells}=12; *RYR1*-p.R163C/ dominant negative TRPC6 n_{cells}=11. Values are expressed as means±S.D. for each condition. Statistical analysis was done using a one-way ANOVA with Tukey's post-test, *$p \leq 0.05$.

Supplementary Figure 2. ***The effect of 1,2-dioctanoyl-sn-glycerol on intracellular calcium and sodium concentration was inhibited by the expression dominant negative TRPC6 channel in single cells muscle fibers,*** Intracellular Ca^{2+} or Na^+ concentration was measured *in vitro* in single FDB muscle fibers isolated from wild type, wild type/dominant negative TRPC6, *RYR1*-p.R163C, and *RYR1*-p.R163C dominant/negative TRPC6 before and after the incubation in 1,2-dioctanoyl-sn-glycerol 100 µM. 1,2-dioctanoyl-sn-glycerol induced elevation of intracellular Ca^{2+} and Na^+ concentration in all genotypes. Expression of dominant negative TRPC6 abolished the robust elevation of intracellular Ca^{2+} or Na^+ concentration upon incubation in 1,2-dioctanoyl-sn-glycerol. The experimental conditions used are indicated on the horizontal axis. N_{mice}=3/genotype, For intracellular Ca^{2+} concentration measurements Wild Type, n_{cells}=11; Wild Type-1-oleoyl-2-acetyl-sn-glycerol n_{cells}=13; Wild Type dominant negative TRPC6, n_{cells}=11; Wild Type dominant negative TRPC6-1-oleoyl-2-acetyl-sn-glycerol n_{cells}=13; *RYR1*-p.R163C n_{cells}=13; *RYR1*-p.R163C-1-oleoyl-2-acetyl-sn-glycerol n_{cells}=16 *RYR1*-p.R163C/ dominant negative TRPC6 n_{cells}=12; *RyR1*-p.R163C/ dominant negative TRPC6-1-oleoyl-2-acetyl-sn-glycerol n_{cells}=10. For intracellular Na^+ concentration measurements N_{mice}=3/genotype, Wild Type, n_{cells}=10; Wild Type-1-oleoyl-2-acetyl-sn-glycerol n_{cells}=11; Wild Type dominant negative TRPC6, n_{cells}=11; Wild Type dominant negative TRPC6-1-oleoyl-2-acetyl-sn-glycerol n=12; *RYR1*-p.R163C n_{cells}=11; *RYR1*-p.R163C-1-oleoyl-2-acetyl-sn-glycerol n=12 *RYR1*-p.R163C/ dominant negative TRPC6 n_{cells}=11; *RYR1*-p.R163C/ dominant negative TRPC6-1-oleoyl-2-acetyl-sn-glycerol n_{cells}=12.Values are expressed as means ± S.D. for each condition. Statistical analysis was done using a one-way ANOVA with Tukey's post-test, *$p \leq 0.05$.

Fig 1

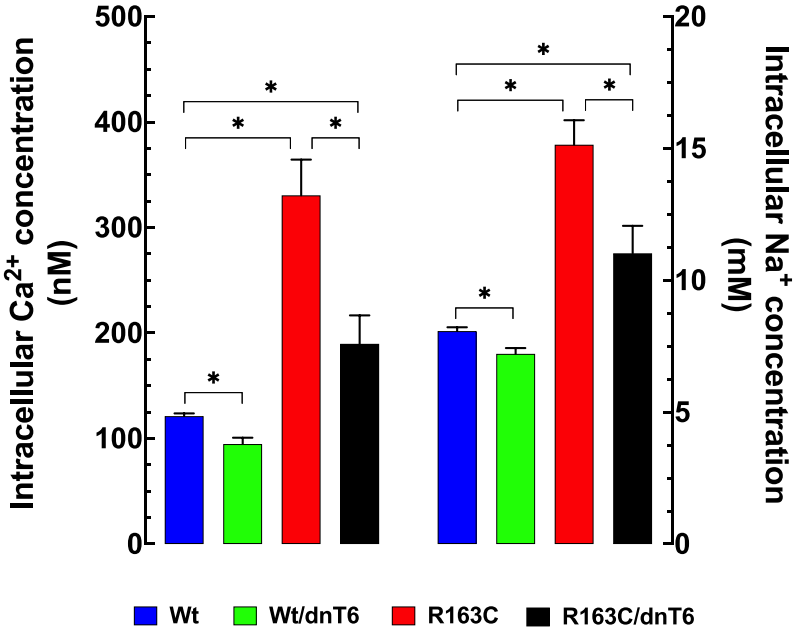
Intracellular Ca2+ concentration (nM)
Intracellular Na+ concentration (mM)
500
400
300
200
100
0
20
15
10
5
0
*
Wt
Wt/dnT6
R163C
R163C/dnT6

Fig 2

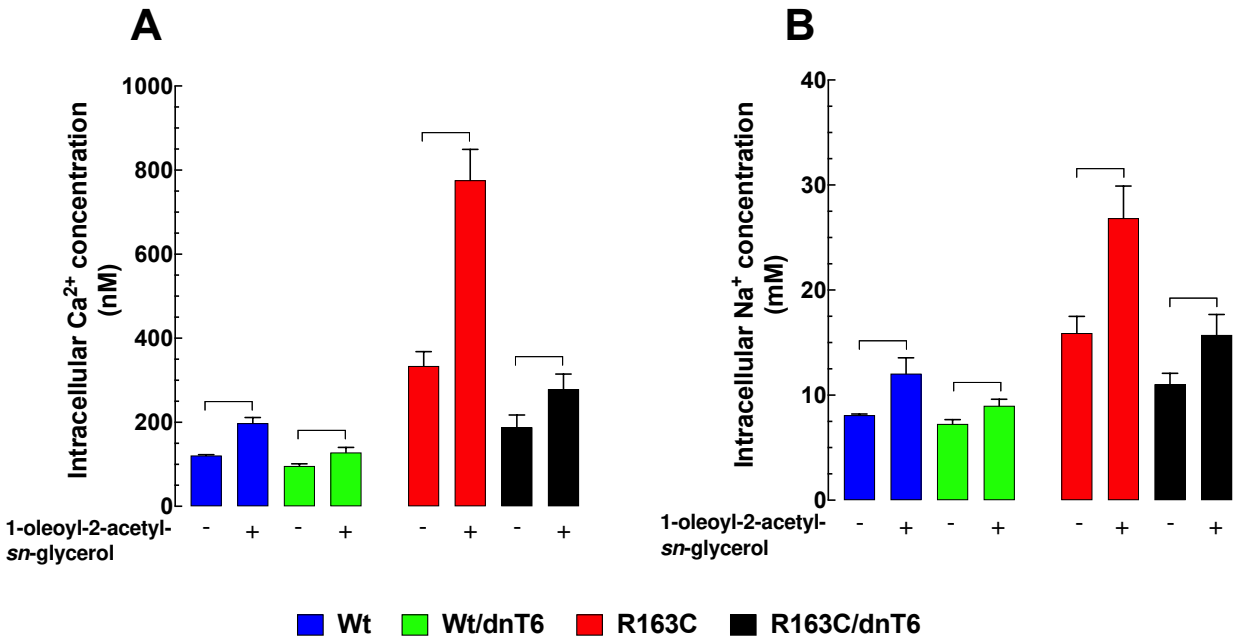
A
B
Intracellular Ca2+ concentration (nM)
Intracellular Na+ concentration (mM)
1000
800
600
400
200
0
40
30
20
10
0
1-oleoyl-2-acetyl-sn-glycerol
- + - + - + - +
Wt
Wt/dnT6
R163C
R163C/dnT6

Fig 3

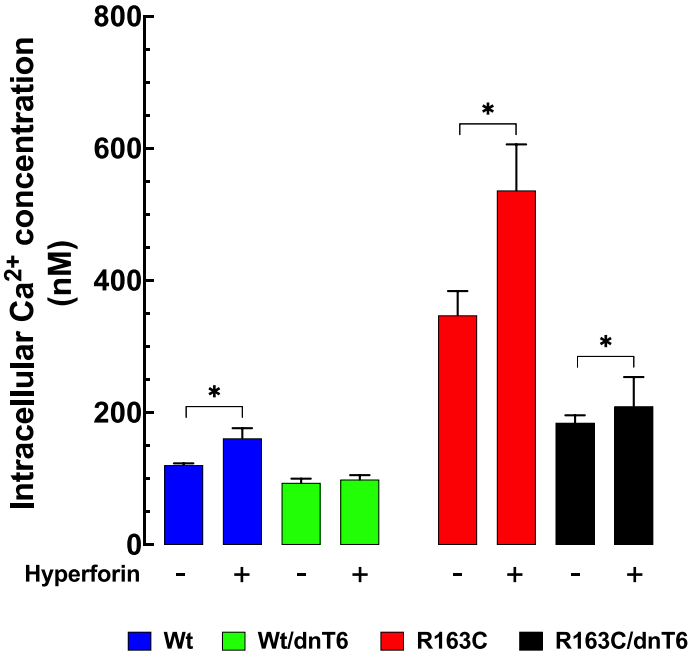
Intracellular Ca2+ concentration (nM)
800
600
400
200
0
*
*
*
Hyperforin - + - + - + - +
Wt
Wt/dnT6
R163C
R163C/dnT6

Fig 4

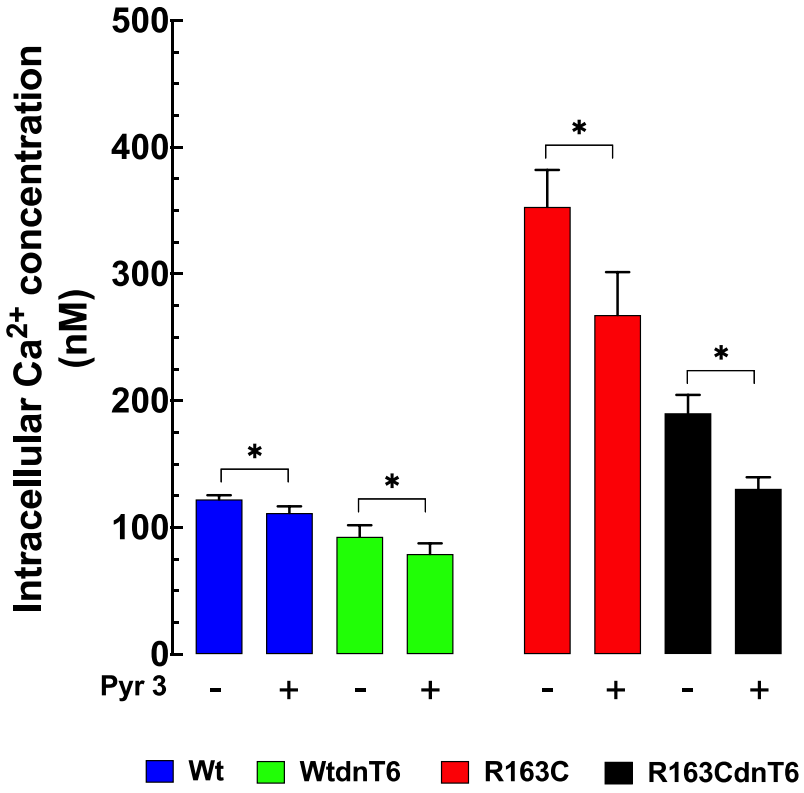
Intracellular Ca2+ concentration (nM)
500
400
300
200
100
0
*
*
*
*
Pyr 3 - + - + - + - +
Wt
WtdnT6
R163C
R163CdnT6

Fig 5

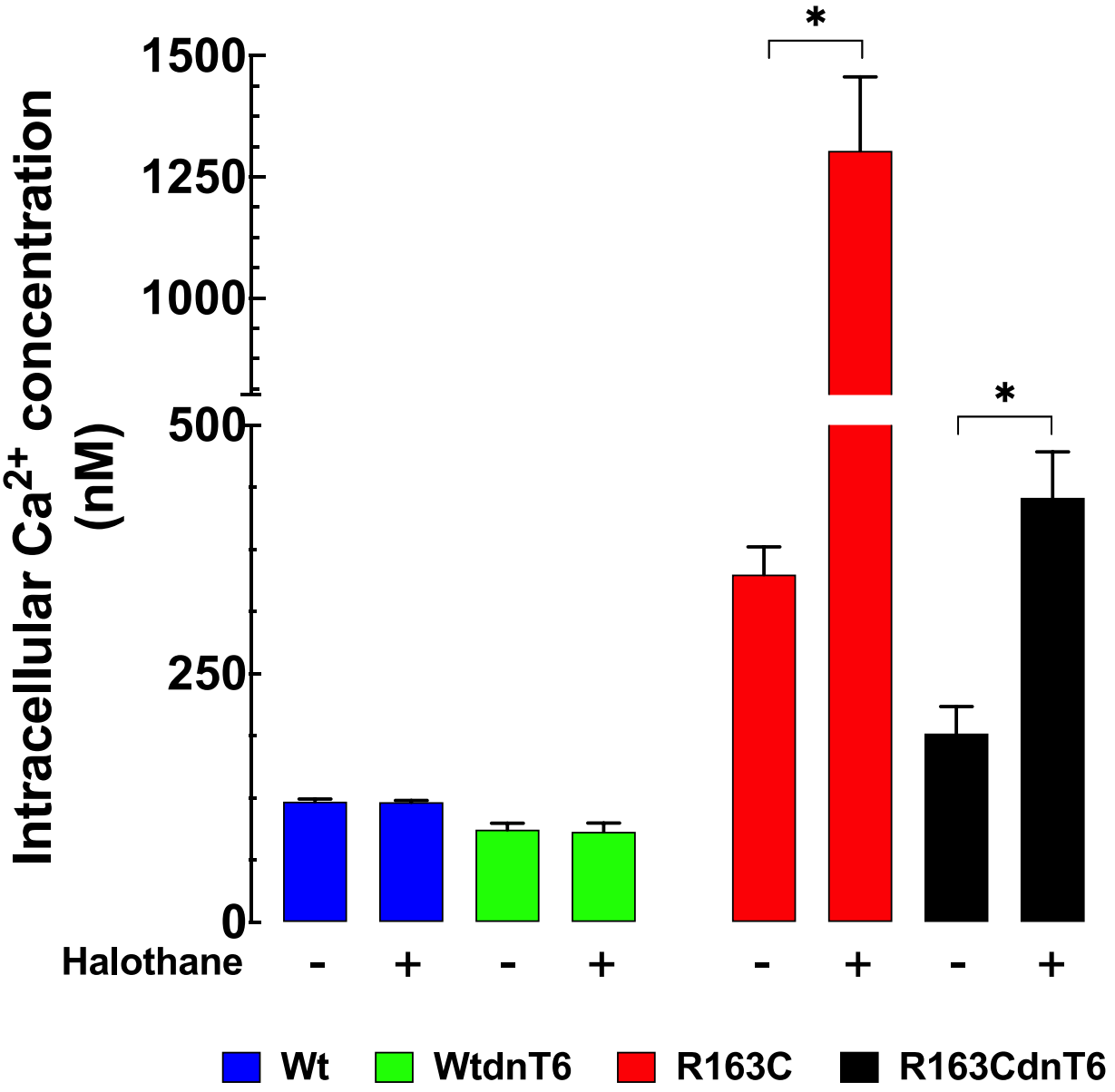
Intracellular Ca^{2+} concentration (nM)
1500
1250
1000
500
250
0
*
*
Halothane
-
+
-
+
-
+
-
+
Wt
WtdnT6
R163C
R163CdnT6

Fig 6

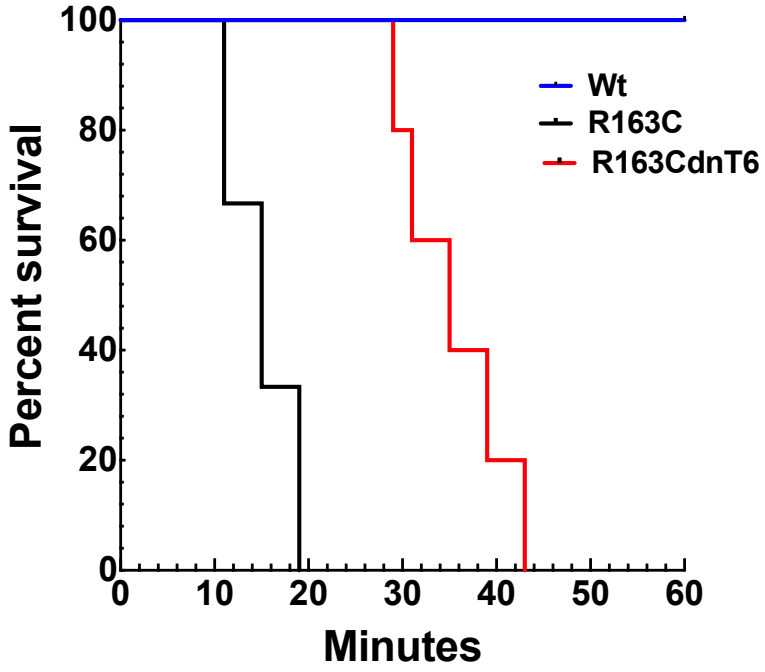
Percent survival
Minutes
Wt
R163C
R163CdnT6
0
20
40
60
80
100
0
10
20
30
40
50
60

Fig 7

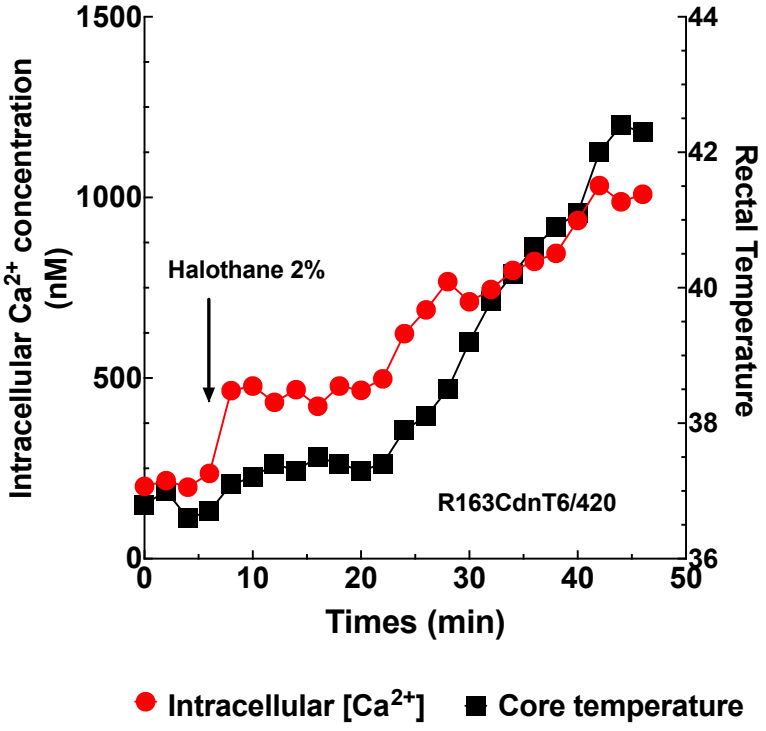
Intracellular Ca2+ concentration (nM)
Rectal Temperature
Times (min)
Halothane 2%
R163CdnT6/420
Intracellular [Ca2+]
Core temperature
0
500
1000
1500
36
38
40
42
44
0
10
20
30
40
50

Fig 8

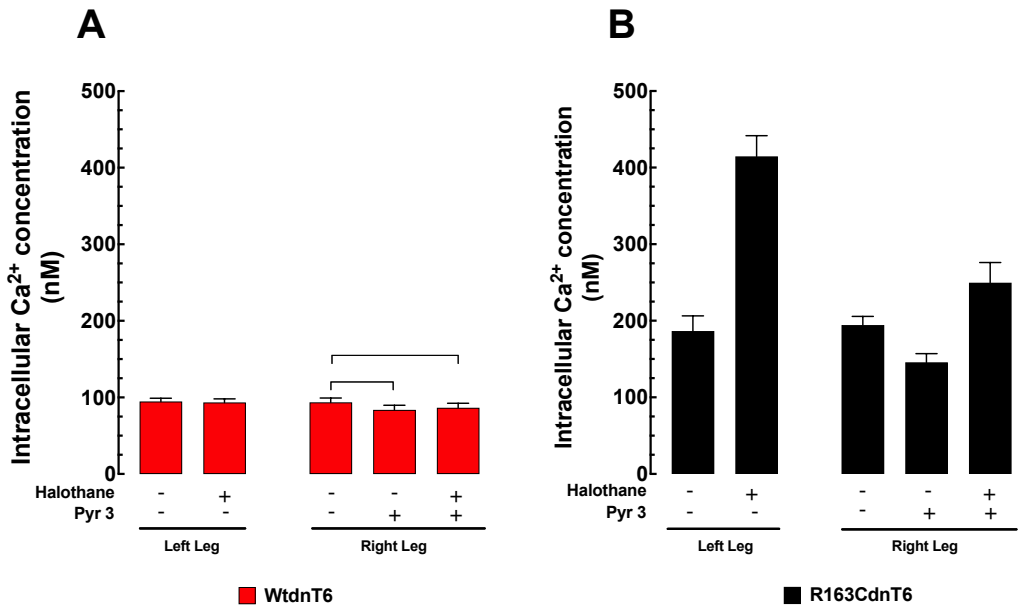
A
B
Intracellular Ca2+ concentration (nM)
500
400
300
200
100
0
Halothane
Pyr 3
- + - - +
- - - + +
Left Leg
Right Leg
WtdnT6
R163CdnT6

Fig 9

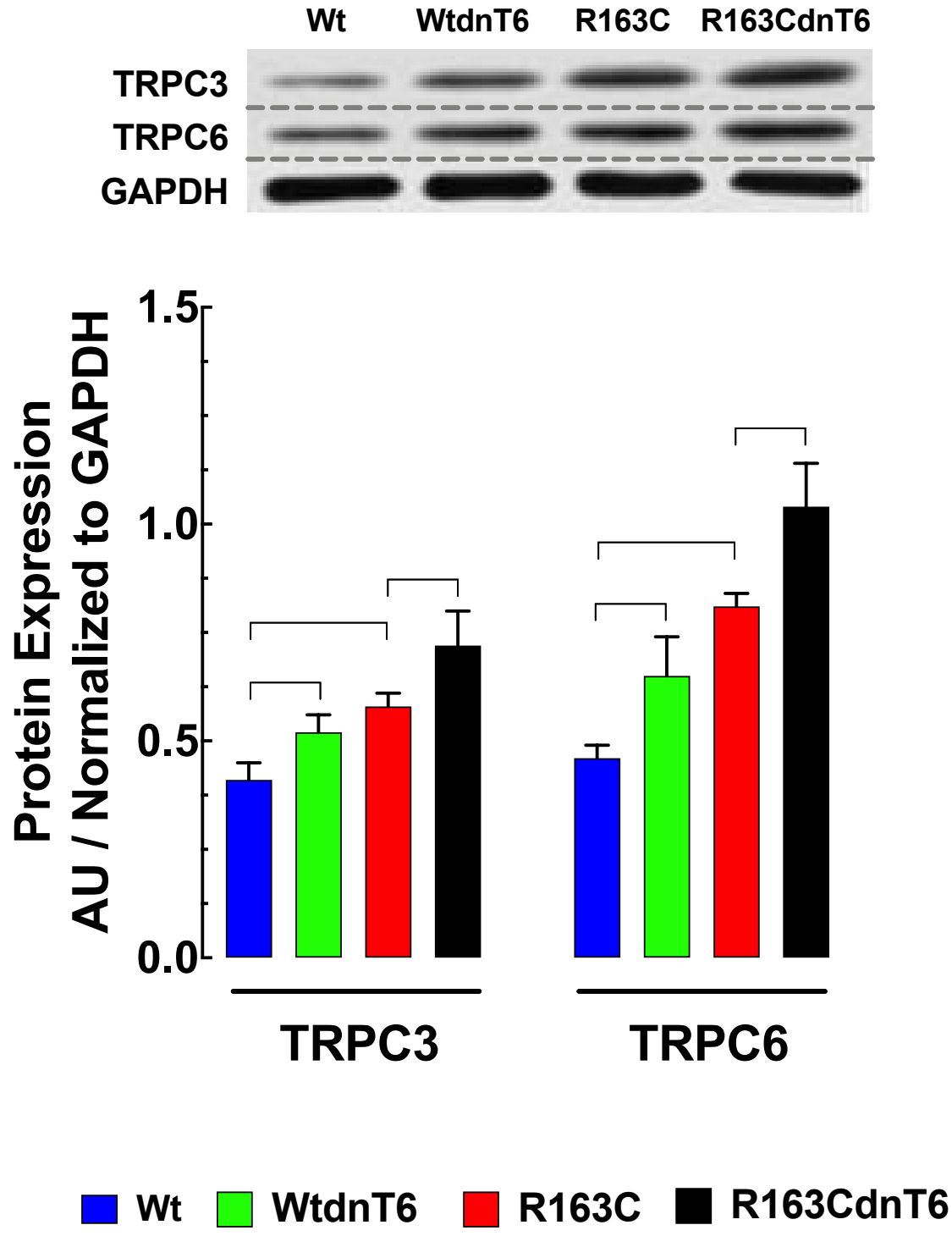
Wt
WtdnT6
R163C
R163CdnT6
TRPC3
TRPC6
GAPDH
Protein Expression
AU / Normalized to GAPDH
1.5
1.0
0.5
0.0
TRPC3
TRPC6
Wt
WtdnT6
R163C
R163CdnT6